

The late Miocene Campo Coy gypsum (Eastern Betics, Spain)

Los yesos del Mioceno superior de Campo Coy (Cordillera Bética oriental, España)

David Artiaga¹, Javier García-Veigas¹, Luis Gibert² and Jesús M. Soria³

¹ CCiTUB Scientific and Technological Centers, Universitat de Barcelona, 08028 Barcelona, Spain; dartiaga@ub.edu; garcia_veigas@ub.edu.

² Departament de Mineralogia, Petrologia i Geologia Aplicada, Universitat de Barcelona, 08028 Barcelona, Spain; lgibert@ub.edu.

³ Departamento de Ciencias de la Tierra y del Medio Ambiente, Universidad de Alicante, Apdo. Correos 99, 03080 Alicante, Spain. jesus.soria@ua.es.

ABSTRACT

The Campo Coy basin contains an important evaporite succession, up to 350 meters thick of gypsum, including two gypsum units: lower and upper gypsum units. These are characterized by fine-grain laminated and selenitic primary gypsums and by nodular-laminated and meganodular secondary gypsums. The geochemical study based on sulfate isotope compositions ($\delta^{34}\text{S}$ and $\delta^{18}\text{O}$) and strontium isotope ratios ($^{87}\text{Sr}/^{86}\text{Sr}$) point to the chemical recycling of Triassic marine evaporites. Isotope compositions ($\delta^{18}\text{O}$ and δD) of the hydration water of gypsum point to continental waters for primary gypsum precipitation. These results are consistent with a shallow lacustrine environment for the Campo Coy gypsum deposit.

Key-words: evaporites, geochemistry, Neogene Betic basins

Geogaceta, 67 (2020), 63-66
ISSN (versión impresa): 0213-683X
ISSN (Internet): 2173-6545

Introduction

The Neogene plate convergence between Iberia and Africa produced the uplift of the Rif and Betic ranges and the narrowing and partial closure of the Atlantic – Mediterranean gateways. During the early-middle Tortonian, these connections between the Mediterranean and the Atlantic occurred by the North Betic and Rif seaways, both corresponding to the foreland basins of the Betic and Rif ranges, respectively.

In the late Tortonian, the progressive Betic uplift and the closure of the Atlantic-Mediterranean connections resulted in several interconnected marine basins that were restricted and isolated at the end of the Tortonian and during the Messinian.

Depending on their palaeogeographic position with regard to the present Mediterranean coast, two main types of Mediterranean-linked basins (in the sense of Braga *et al.*, 2003) are distinguished: the “marginal basins” near the present-day Mediterranean sea, and the “inner basins” distant from the present-day Mediterranean coast. The “marginal ba-

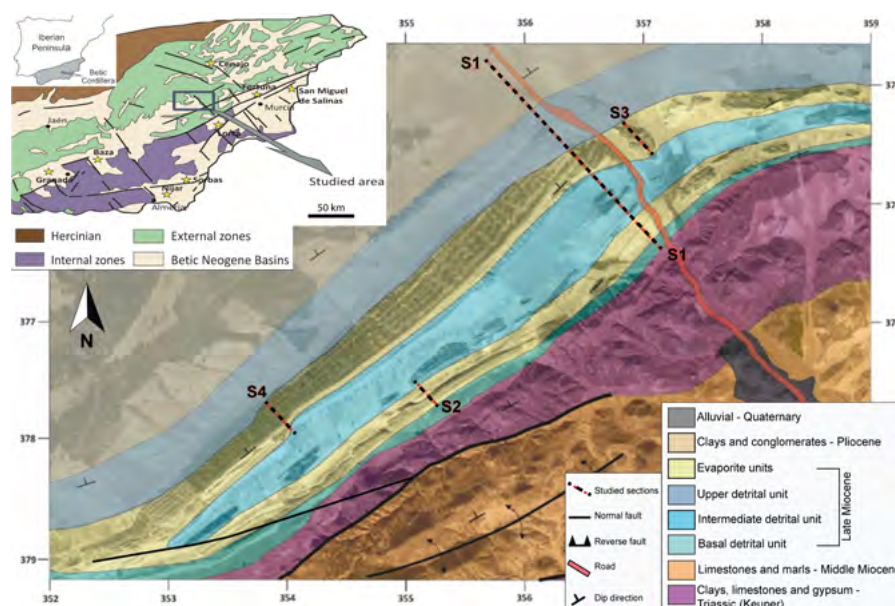


Fig. 1.- Geological map of the Campo Coy basin with location of the studied sections.

Fig. 1. Mapa geológico de la cuenca de Campo Coy con la localización de las secciones estudiadas.

sins”, such as Sorbas, Níjar and Bajo Segura, hosted marine evaporite deposits assigned to the Messinian Salinity Crisis (e.g., Rouchy, 1982; Riding *et al.*, 1998, Rouchy and Caruso, 2006, García-Veigas *et al.*, 2018). In the “inner basins”, whose positions is currently more inland, the

evaporitic formations were formed during late Tortonian and early Messinian ages in continental or transitional conditions, from marine to continental, as occurs in the basins of Granada, Lorca and Fortuna (Playà *et al.*, 2000; García-Veigas *et al.*, 2013, 2019).

The present study is focused on the stratigraphy, petrology and geochemistry of the evaporite succession of the Campo Coy basin, one of the most internal Neogene Betic basins. The aim is to understand the origin of this evaporite succession and to characterize the sedimentary environment where evaporites formed.

Geological setting and studied material

The Campo Coy basin is a long, rectangular basin, ~8 km long and ~2 km

wide, located between the Lorca and Caravaca villages (Murcia). The basement is made up of allochthonous rocks from the Subbetic domain. The evaporite succession is limited to the north by Pliocene deposits and to the south by Triassic materials (Fig. 1).

The studied gypsum deposit of the Campo Coy basin includes two gypsum units: a lower unit, 100 meters thick, and an upper unit, up to 250 meters thick, both separated by detrital sediments. Geochemical analyses of sulfate isotope compositions ($\delta^{34}\text{S}$ and $\delta^{18}\text{O}$), strontium

isotope ratios ($^{87}\text{Sr}/^{86}\text{Sr}$) and the isotopic composition of the hydration water of gypsum ($\delta^{18}\text{O}$ and δD) have been carried out with the aim of recognizing the chemical evolution of the evaporitic environment and the water source in the Campo Coy basin during gypsum deposition.

Sample material and methods

Four stratigraphic sections have been logged and sampled in the Campo Coy basin (Fig. 1). Mineralogical and textural identification of 25 hand samples and thin sections of gypsum and carbonates has been carried out using petrographic and electronic (ESEM-EDS) microscopes. The micropaleontological identification has been based on more representative and abundant species taken from marly sediments. Each sample was washed over a 170 μm sieve and the residue was directly studied under electronic (ESEM) microscope.

Sulfur and oxygen isotope compositions ($\delta^{34}\text{S}_{\text{CDT}}$ and $\delta^{18}\text{O}_{\text{SMOW}}$) of 31 gypsum samples have been determined at the CCIUB (Barcelona, Spain). Isotope determinations have been performed with a Thermo Finigan Delta Plus XP Spectrometer. The analytical error (2σ) is $\pm 0.3\text{‰}$ for both $\delta^{34}\text{S}$ and $\delta^{18}\text{O}$. Values obtained for the international standard NBS-127 are $\delta^{34}\text{S}$: $20.3 \pm 0.1\text{‰}$, and $\delta^{18}\text{O}$: $9.3 \pm 0.2\text{‰}$ respectively.

Strontium isotope ratios ($^{87}\text{Sr}/^{86}\text{Sr}$) of gypsum samples ($n=5$) have been measured in the CSIRO (North-Ryde, Australia) on a VG 354 TIMS with a long-term analytical precision of ± 0.000014 measured on NBS-987 ($^{87}\text{Sr}/^{86}\text{Sr}$: 0.710235 ± 0.000014). $^{87}\text{Sr}/^{86}\text{Sr}$ ratios have been normalized to $^{86}\text{Sr}/^{88}\text{Sr} = 0.1194$.

Gypsum samples ($n=16$) were also analyzed for $\delta^{18}\text{O}$ and δD of hydration water of gypsum at the CCIUB (Barcelona, Spain). The results are reported as $\delta^{18}\text{O}$ and δD with an analytical precision of $\sim 0.1\text{‰}$ and $\sim 0.8\text{‰}$ respectively.

Stratigraphy and sedimentary facies

In the Miocene filling of the Campo Coy basin, detrital marls and evaporites are the predominant facies. From the analysis of these lithofacies, five units are distinguished (Fig. 2): basal detrital unit, lower gypsum unit, intermediate detrital unit, upper gypsum unit and upper detrital unit.

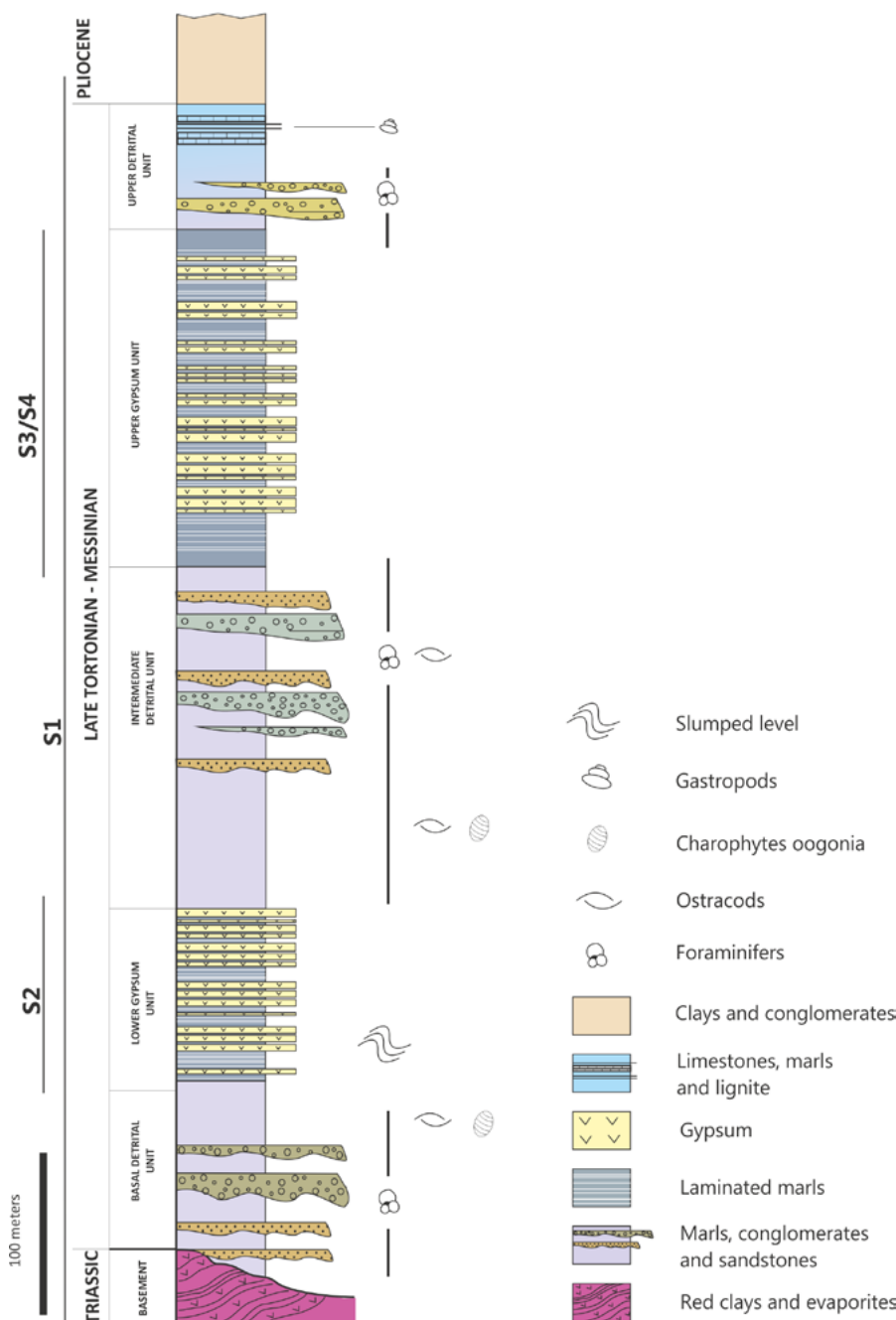


Fig. 2.- General stratigraphic section of the Campo Coy basin. Five units are differentiated in this section based on lithology and sedimentary features.

Fig. 2.- Columna estratigráfica general de la cuenca de Campo Coy. Se han diferenciado cinco unidades en función de la litología y las características sedimentarias.

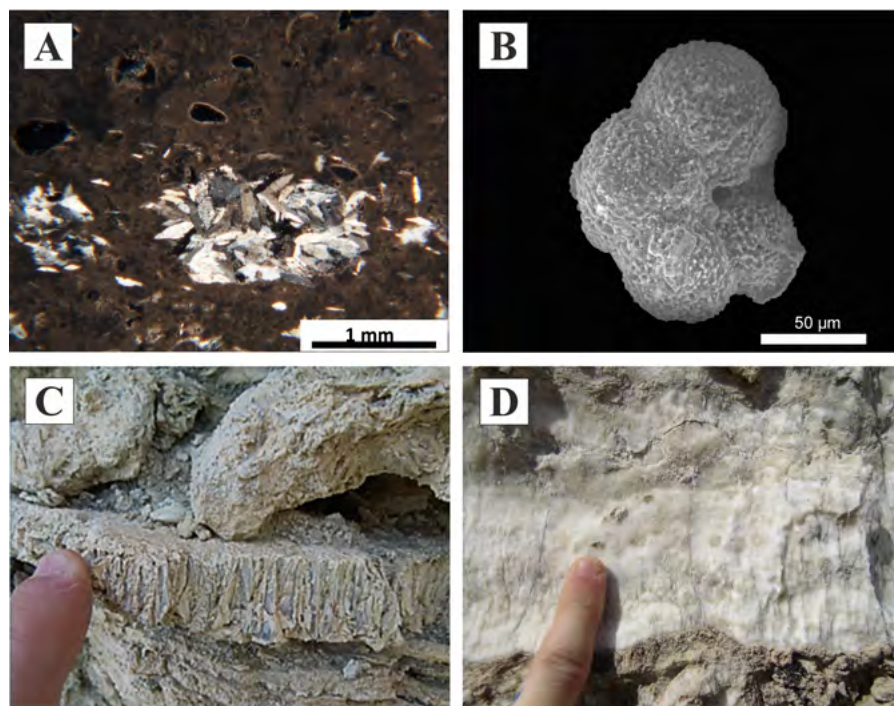


Fig. 3- A) Petrographic image of cumulated lenticular crystals and ostracods shells surrounded by micritic matrix. B) SEM image of *Neogloboquadrina* spp. *sinistral*. C) Selenite gypsum lithofacies from the upper gypsum unit. D) Nodular-laminated gypsum lithofacies from the upper gypsum unit.

Fig. 3. A) Imagen petrográfica de cristales lenticulares de yeso junto con ostrácodos dentro de una matriz micrítica. B) Neogloboquadrina spp. sinistral (imagen de SEM). C) yeso selenítico de la unidad de yesos superior. D) Litofacies de yeso nodular-laminado de la unidad de yesos superior.

Detrital units consist of grey marls with several conglomerate and sandstone bars interbedded. In these detrital units, abundant *in situ* ostracod shells (Fig. 3A), charophytes oogonia and variable reworked planktonic foraminifera have been identified. The foraminifera content is predominantly formed by *Globorotalia scitula* group, *Globorotalia menardii* group and *Neogloboquadrina* spp. (*sinistral* and *dextral* forms) (Fig. 3B), among others. A similar fauna has been described in the Lorca basin and assigned to a late Tortonian age (Corbí *et al.*, 2012). According to these data, the source of these reworked foraminifera could correspond to the eroded late Tortonian materials from surrounding areas. The upper part of the upper detrital unit grades to marls and limestones with some lignite levels rich in gastropods and corresponds to the latest Miocene lacustrine materials (Bruijn *et al.*, 1975). Pliocene materials are overlying the described Campo Coy succession.

The lower gypsum unit consists of primary gypsum beds, ranging from few millimeters to few centimeters thick, composed of fine-grained laminated and selenite gypsum lithofacies (Fig 3C). Selenite crystals are up to 5 cm long. Some levels of secondary macrocrystalline and

nodular gypsum also occur towards the top of the unit.

The upper gypsum unit contains eight evaporite levels (~15 meters thick each one) separated by laminated marls (~3 meters thick). The first three levels are the most complete and consist of primary and secondary gypsum beds. Primary gypsum dominates at the base of the lower gypsum levels and shows three main lithofacies: fine-grained laminated gypsum, selenite gypsum with gypsum crystals reaching up to 5cm in length, and cumulated gypsum. The upper evaporite levels are poorly exposed and mainly composed of nodular-laminated (Fig. 3D) and meganodular secondary gypsum.

Geochemistry of gypsum

Sulfate isotope compositions ($\delta^{34}\text{S}$ and $\delta^{18}\text{O}$) for late Miocene marine evaporites are close to 22‰ and 12‰ respectively (Claypool *et al.*, 1980; Paytan *et al.*, 1998; Turchyn and Schrag, 2004; Kampschulte and Strauss, 2004; García-Veigas *et al.*, 2018). $^{87}\text{Sr}/^{86}\text{Sr}$ isotope ratios between 0.708800 and 0.709100 should be expected for late Miocene marine evaporites (Veizer *et al.*, 1999; Korte *et al.*, 2003, and others).

Sulfur isotope compositions of the Campo Coy gypsum show very homogeneous values ranging between +13.8‰ and +15.6‰. Oxygen isotope compositions also show quite homogeneous values with variations from +13.8‰ to +18.7‰. These values do not match with expected values for late Miocene marine evaporites. Comparing these data with published isotopic ranges from Triassic marine evaporites in the Betics (12‰-17‰ for $\delta^{34}\text{S}$, and 8‰-18‰ for $\delta^{18}\text{O}$ at Ortí *et al.*, 2014), we interpret that the source of the dissolved sulfate in the Campo Coy gypsum precipitating waters is the recycling of Triassic evaporites (Fig. 4).

The strontium isotope ratios ($^{87}\text{Sr}/^{86}\text{Sr}$) of the lower and the upper gypsum units range between 0.707788 and 0.707888, far from expected for late Miocene marine deposits. These values fall within the range of Triassic marine evaporites. In agreement with the sulfate isotope compositions, the strontium isotope ratios ($^{87}\text{Sr}/^{86}\text{Sr}$) of the Campo Coy gypsum point to the contribution of recycled strontium from marine Triassic rocks in the Betic range.

During precipitation, the hydration water of gypsum is enriched in the heaviest oxygen isotope (^{18}O) and depleted in deuterium (^2H) with respect to the parent waters. Fractionation factors of 1.004 and 0.981, for oxygen and deuterium respectively (Gázquez *et al.*, 2017), have been used to recognize the isotopic compositions of the parent waters. Following corrections, the calculated $\delta^{18}\text{O}$ of parent waters for primary gypsum ranges from 0.1‰ to 3.3‰, and from -7.5‰ to -4.4‰ for secondary gypsum. The-calculated δD values of parent waters for primary gypsum range between -1.7‰ and -12.9‰, and between -28.3‰ and -40.0‰ for secondary gypsum. The $\delta^{18}\text{O} - \delta\text{D}$ diagram (Fig. 5) shows that the isotopic values of the hydration waters for primary gypsum and their predicted parent waters correspond with a non-marine paleolake environment whereas the isotopic signature of secondary gypsum agrees with the present-day meteoric water trend reported in the eastern Betics.

Discussion

The lack of *in situ* biomarkers within the detrital units below and between the Campo Coy evaporites does not allow us to assign a specific age for this

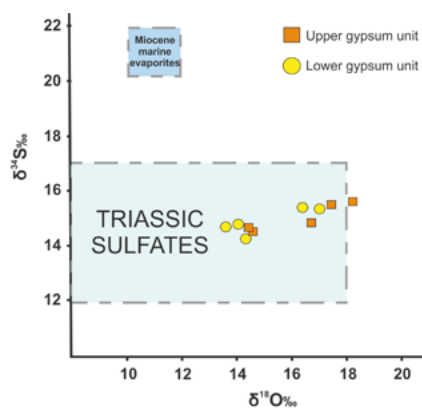


Fig. 4.- Sulfate isotope composition of the lower and upper gypsum units. The shaded area of Triassic values is taken from Ortí et al. (2014). See the text for references to isotopic data.

Fig. 4. Composición isotópica del sulfato de las unidades de yeso inferior y superior. El área correspondiente a los valores isotópicos de sulfatos triásicos se ha tomado de Ortí et al. (2014). Ver el texto para las referencias de datos isotópicos.

gypsum deposit. However, taking into account the overlying Pliocene materials and the presence of late Tortonian reworked foraminifera within the intercalated detrital sediments, we can suggest that the Campo Coy gypsum precipitated during the late Tortonian – Messinian.

The geochemical signature of the Campo Coy gypsum deposit is similar to that found in non-marine evaporites formed in other internal Neogene Betic basins such as Lorca and Fortuna basins (García-Veigas et al., 2019).

Conclusions

The gypsum units of Campo Coy precipitated in a shallow lacustrine environment. Variations in the water balance of the basin controlled the type of deposited sediments. Periods with higher runoff lead to the deposition of detrital sediments while gypsum precipitation took place during drier periods with less continental water input.

Although the age of the evaporitic sedimentation is still unclear, it could be assigned to the late Tortonian – Messinian.

Acknowledgements

This study was supported by the projects CGL-2013-42689 and CGL2016-79458 of the Spanish Government. The authors are also indebted to J. Illa, R.M. Marimón, E. Aracil (UB) and D.I. Cendón (ANSTO) for their technical support. We would also like to thank the reviewers H. Corbí and J.M. Martín Martín for their corrections which improved the final version of the text.

References

Braga, J.C., Martín, J.M. and Quesada, C. (2003). *Geomorphology* 50, 3-26.
 Bruijn, H. de, Mein, P., Montenat, C. and Van De Weerd, A. (1975). *Proc. Kon. Ned.*

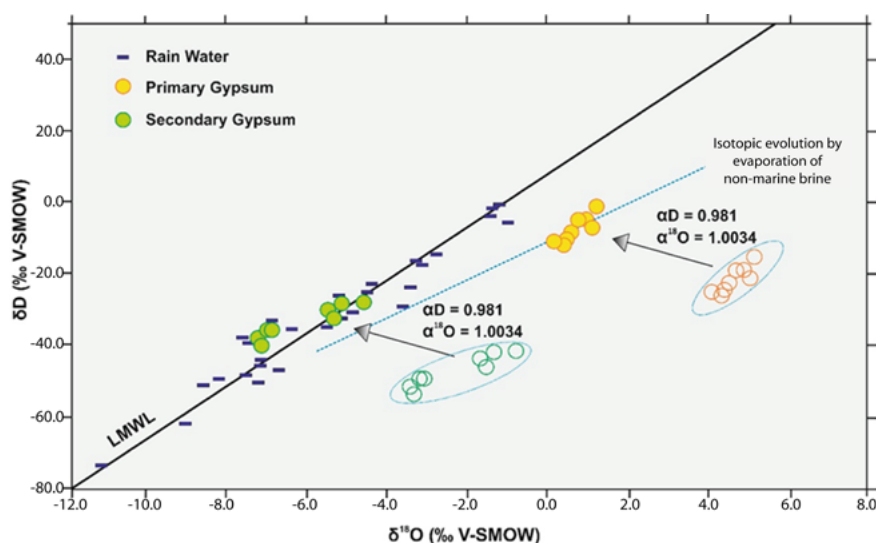


Fig. 5.- Diagram of $\delta^{18}O$ and δD of hydration water from Campo Coy primary gypsum (filled yellow circles) and secondary gypsum (filled green circles) after correction for fractionation factor; the rain water (dashes) data are taken from REVIP of Spanish Government.

Fig. 5. Diagrama $\delta^{18}O$ and δD del agua de hidratación del yeso primario (círculos amarillos rellenos) y yeso secundario (círculos verdes rellenos) después de aplicar los factores de corrección de fraccionamiento isotópico; los valores de agua de lluvia (segmentos) han sido tomados de REVIP, Gobierno de España.

Akad. van Wetensch. 78, 1-32.

Claypool, G.E., Holser, W.T., Kaplan, I.R., Sakai, H. and Zak, I. (1980). *Chemical Geology* 28, 199–260.

Corbí, H., Lancis, C., García-García, F., Pina, J.A., Soria, J.M., Tent-Manclús, J.E. and Viseras, C. (2012). *Geobios* 45, 249–263.

García-Veigas, J., Cendón, D., Rosell, L., Ortí, F., Torres Ruiz, J., Martín, J.M. and Sanz, E. (2013). *Palaeogeography, Palaeoclimatology, Palaeoecology* 369, 452–465.

García-Veigas, J., Cendón, D., Gibert, L., Lowenstein, T.K. and Artiaga, D. (2018). *Marine Geology* 403, 197-214.

García-Veigas, J., Gibert, L., Cendón, D., Artiaga, D., Corbí, H., Soria, J.M., Lowenstein, T.K. and Sanz, E. (2019). *Basin Research* DOI: 10.1111/bre.12408

Gázquez, F., Evans, N. and Hodell, D.A. (2017). *Geochimica et Cosmochimica Acta* 198, 259-270.

Kampschulte, A. and Strauss, H. (2004). *Chemical Geology* 204, 255–286.

Korte, C., Kozur, H.W., Bruckschen, P. and Veizer, J. (2003). *Geochimica et Cosmochimica Acta*, 67, 47– 62

Paytan, A., Kastner, M., Campbell, D. and Thiemens, M.H. (1998). *Science* 282, 1459–1462.

Playà, E., Ortí, F. and Rosell, L. (2000). *Sedimentary Geology* 133, 135–166.

Riding, R., Braga, J.C., Martín, J.M. and Sánchez-Almazo, I.M. (1998). *Marine Geology* 146, 1-20.

Rouchy J.M. (1982). *La genèse des évaporites messiniennes de Méditerranée*. Mémoire du Muséum National d’Histoire Naturelle de Paris, NS, série C, L, 267 p.

Rouchy, J.M. and Caruso, A. (2006). *Sedimentary Geology* 188-189, 35-67.

Turchyn, A.V. and Schrag, D.P. (2004). *Science* 303, 2004-2007.

Veizer, J., Ala, D., Azmy, K., Bruckschen, P., Buhl, D., Bruhn, F., Carden, G.A.F., Diener, A., Ebner, S., Godderis, Y., Jasper, T., Korte, Ch., Pawellwk, F., Podlaha, O. and Strauss, H. (1999). *Chemical Geology* 161, 59-88